

Supplement of Atmos. Chem. Phys., 16, 12513–12529, 2016  
<http://www.atmos-chem-phys.net/16/12513/2016/>  
doi:10.5194/acp-16-12513-2016-supplement  
© Author(s) 2016. CC Attribution 3.0 License.



Atmospheric  
Chemistry  
and Physics  
Open Access  
EGU

*Supplement of*

## **Chemical ionization of clusters formed from sulfuric acid and dimethylamine or diamines**

**Coty N. Jen et al.**

*Correspondence to:* Coty N. Jen ([jenco@berkeley.edu](mailto:jenco@berkeley.edu))

The copyright of individual parts of the supplement might differ from the CC-BY 3.0 licence.

## Supporting Information:

- S1. Mass-dependent sensitivity of the Cluster CIMS
- S2. Nitrate vs. acetate mass spectra comparison for sulfuric acid+diamine
- S3.  $[N_1]$  and  $[N_2]$  from mass spectrometer signals
- S4. Modeled reactions and parameters

### S1. Mass-dependent sensitivity of the Cluster CIMS:

Mass-dependent sensitivity experiments were performed on the University of MN Cluster CIMS following a near identical procedure as detailed in Zhao et al. (2010), with pertinent details described here. Four tetra-alkyl ammonium halide salts were used in this experiment: tetramethyl ammonium iodide (TMAI at 74 and 275 amu), tetrapropyl ammonium iodide (TPAI at 186 amu), tetrabutyl ammonium iodide (TBAI at 242 amu), and tetraheptyl ammonium bromide (THAB at 410 amu). These salts were dissolved in methanol and electrosprayed in positive ion mode. Specific ion mobilities (Ude and de la Mora, 2005) were selected using a high resolution differential mobility analyzer (HDMA) (Rosser and de la Mora, 2005). The flow containing mono-mobile ions was split into two equal streams with one measured by an electrometer and the other by the Cluster CIMS. The ions were directly delivered to the inlet of the Cluster CIMS where they first entered a conical octopole (1 MHz and 24 V pk-pk) then the quadrupole mass analyzer. The signals of the Cluster CIMS were then divided by the electrometer measured concentrations to obtain the sensitivity. Since the ions were delivered directly to the Cluster CIMS inlet, these experiments only probe the mass-dependent sensitivity of the inlet, octopole, quadrupole, and detector.

Figure S1 shows measured sensitivity at specific masses corresponding to the alkyl halide positive ions (black squares). We assume the mass-dependent sensitivity for positive ions is the same for negative ions. The sensitivity at smaller masses is lower than at larger masses, indicating that the Cluster CIMS more efficiently measures larger ions. For masses between 410 to 710 amu, we assume a sensitivity value of  $0.037 \text{ Hz cm}^{-3}$  (green line). Masses larger than 710 amu are not detected (i.e., sensitivity of zero) due to limits of our quadrupole. A constant sensitivity assumes that all mass from ~200-710 amu are measured with equal efficiency. This contrasts with Zhao et al. (2010) where they observed a steep decline in sensitivity at large masses. We based our assumption on the size and shape of largest mass peaks. Figure S2 shows a sample mass scan of sulfuric acid with  $[EDA]=60 \text{ pptv}$ . The largest ion detected is  $A_6 \cdot EDA_2$  at 707 amu. The peak is ~4 amu wide and ~600 Hz tall. If the sensitivity for this large ion were low, then the resulting  $[A_6 \cdot EDA_2]$  would exceed that of  $[A_2^-]$ , an unlikely scenario.

The uncertainties associated with the sensitivity depend on the ion masses being compared. For ions similar in mass, such as  $HNO_3 \cdot NO_3^-$  (125 amu) and  $HNO_3 \cdot HSO_4^-$  (160 amu), the uncertainty is small at ~20%. However, taking the ratio between various sulfuric acid clusters and the acetate reagent ion signals can result in uncertainties up to a factor of 2 to 3. This large uncertainty is due to extrapolating between the two smallest ion masses studied in the sensitivity measurements: 74 to 186 amu. In addition, the acetate reagent ions are all very small and fall on

the steep rise of the sensitivity curve. More sensitivity experiments are required in the low mass range to reduce this uncertainty.

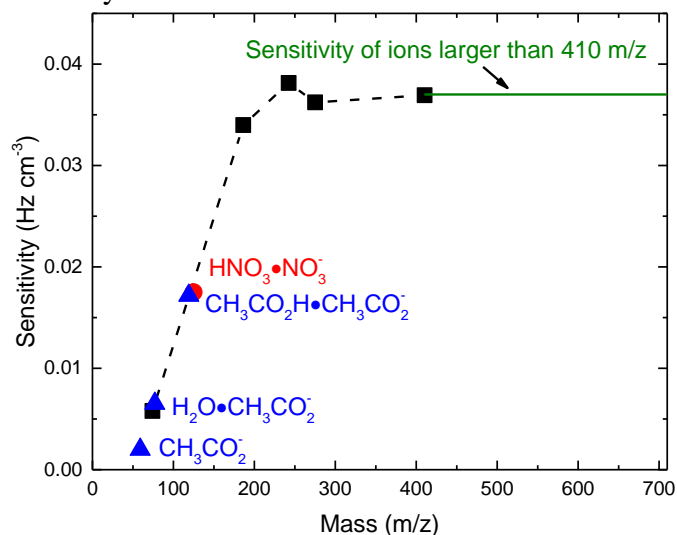


Figure S1 Sensitivity of the UMN Cluster CIMS as a function of mass. The black squares indicate the measured sensitivity of the positive alkyl halide ions. The blue triangles show the predicted sensitive of the acetate ions with three different ligands. The red circle is the sensitivity of the nitrate dimer ion. The dark green line is the extrapolated sensitivity for masses larger than 410 amu.

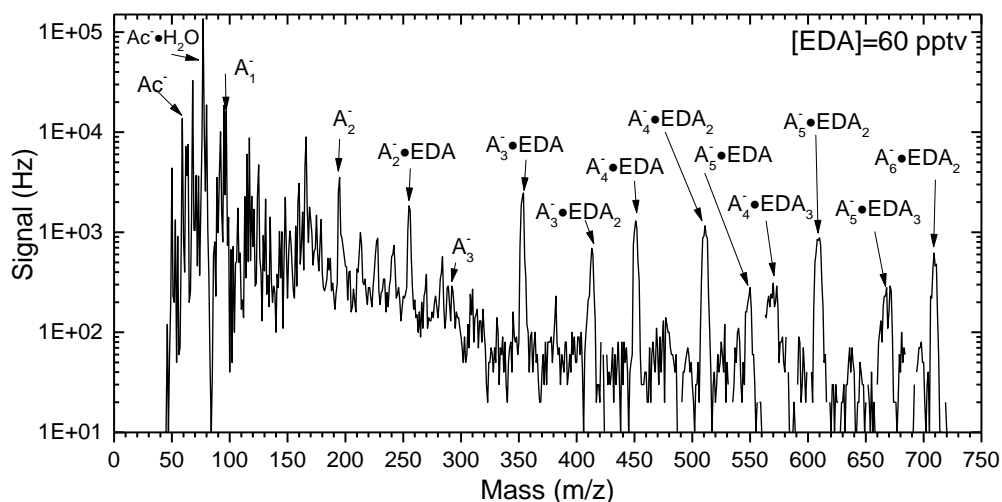


Figure S2 Mass scan of sulfuric acid at  $[A_1]_0=4 \times 10^9 \text{ cm}^{-3}$  and  $[\text{EDA}]=60 \text{ pptv}$  measured using acetate ( $\text{Ac}^-$ ). Identities of sulfuric acid+EDA peaks are labeled.

## S2. Nitrate vs. acetate mass spectra comparison for sulfuric acid+diamine

Figure S3 compares nitrate and acetate mass spectra for the three diamines at equivalent  $[A_1]_0$  and  $[\text{B}]$ . As no other parameters of the Cluster CIMS changed between nitrate and acetate measurements, Figure S3 clearly shows that nitrate does not chemically ionize all types of sulfuric clusters in the presence of diamines. It is possible that larger ion clusters decompose to a greater extent with acetate CI than nitrate and lead to increased signal for the clusters shown in Figure S3. However, normalized acetate signals are 10 times larger than nitrate signals which

would require very high and nonsensical concentrations of the larger clusters for decomposition to be the sole reason for the difference. Furthermore, nitrate detects small amounts of  $A_3^- \bullet \text{diamine}$ ; this could be due to decomposition of larger ions, IIC from  $N_2 + A_1^-$ , or partially efficient nitrate CI of  $A_3^- \bullet \text{diamine}$ .

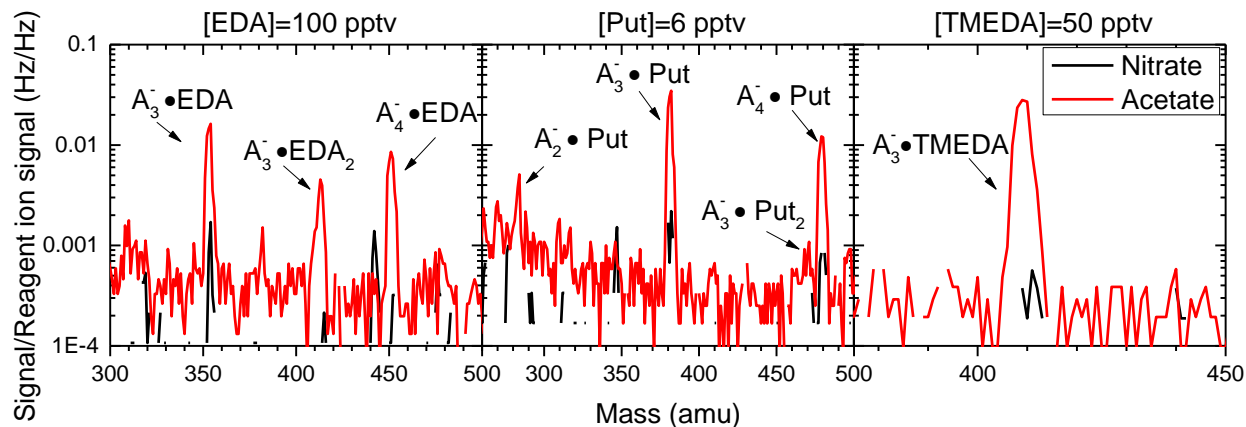


Figure S3 Comparison between nitrate (black) and acetate (red) mass spectra for EDA (left), Put (center), and TMEDA (right). The concentration of diamine for the comparison is given at the top of each panel.

### S3. $[N_1]$ and $[N_2]$ from mass spectrometer signals

The depletion of the reagent ion (given here as  $[NO_3^-]$ ) can be written as

$$\frac{d[NO_3^-]}{dt_{CI}} = -k_1 [N_1] [NO_3^-] \quad \text{Equation S1}$$

This assumes that the reagent ion only reacts with  $N_1$ . This has a solution of

$$[NO_3^-] = [NO_3^-]_o \exp(-k_1 [N_1] t_{CI}) \quad \text{Equation S2}$$

Assuming  $[A_1^-]$  is not formed in appreciable quantities by ion fragmentation, then the formation of  $[A_1^-]$  can be written as

$$\frac{d[A_1^-]}{dt_{CI}} = k_1 [N_1] [NO_3^-] - k_{21} [A_1^-] [N_1] \quad \text{Equation S3}$$

Substituting Equation S2 into Equation S3 gives

$$\frac{d[A_1^-]}{dt_{CI}} = k_1 [N_1] [NO_3^-]_o \exp(-k_1 [N_1] t_{CI}) - k_{21} [A_1^-] [N_1] \quad \text{Equation S4}$$

Where  $[\text{NO}_3^-]_o$  is the initial concentration of  $\text{NO}_3^-$ . Equation S4 can be solved to give

$$[A_1^-] = k_1 [\text{NO}_3^-]_o \left( \frac{\exp(-k_1 [N_1] t_{CI}) - \exp(-k_{21} [N_1] t_{CI})}{k_{21} - k_1} \right) \quad \text{Equation S5}$$

Equation S2 can be inserted in Equation S5 to remove  $[\text{NO}_3^-]_o$ .

$$\frac{[A_1^-]}{[\text{NO}_3^-]} = \frac{S_{160}}{S_{125}} = \frac{k_1}{k_{21} - k_1} (1 - \exp((k_1 - k_{21}) [N_1] t_{CI})) \quad \text{Equation S6}$$

The signal at the ion's mass directly relates to the ion concentration (plus a mass-dependent sensitivity that we do not include in this derivation for simplicity but is included in the model); therefore, the  $[A_1^-]$  can be replaced by  $S_{160}$  (bisulfate with a nitric acid ligand with a total mass of 160 amu) and  $[\text{NO}_3^-]$  with  $S_{125}$  (nitrate with a nitric acid ligand for a mass of 125 amu). Equation S6 is a more accurate method to convert signal ratios to neutral concentration than the equations given in Berresheim et al. (2000) and Eisele and Hanson (2000) as this equation does not assume constant concentrations of the reagent ion. However, at very short  $t_{CI}$  (like the 15 to 18 ms used here), Equation S6 results in  $[N_1]$  about 5% higher than using the logarithmic equation given in Berresheim et al. (2000) and 1% higher than the simple ratio equation of Eisele and Hanson (2000).

The derivation for  $[A_2^-]$  ( $S_{195}$ ) follows similar math as for  $[A_1^-]$ . The relation for  $[A_2^-]$  as a function of  $t_{CI}$  is given in Equation S7 and can be divided by Equation S5 to obtain  $S_{195}/S_{160}$  vs.  $t_{CI}$  (not shown).

$$[A_2^-] = \frac{k_{21} k_1}{k_{21} - k_1} [\text{NO}_3^-]_o \left\{ \begin{array}{l} \exp(-k_1 [N_1] t_{CI}) / (k_{32} - k_1) + \exp(-k_{21} [N_1] t_{CI}) / (k_{21} - k_{32}) \\ - \exp(-k_{32} [N_1] t_{CI}) / ((k_{32} - k_1)(k_{21} - k_{32})) \end{array} \right\} \quad \text{Equation S7}$$

Ratio of cluster signals to the reagent ion can be affected by several factors not considered in Equation S6. 1) Varying relative humidity alters the number of water ligands attached to charged and neutral clusters. This will alter the kinetics and stability of clusters, thus changing the amount and types of clusters detected. 2) The addition of base into the flow reactor introduces a small stream of nitrogen that may locally dilute  $[N_1]$  by up to 40% with very high base addition flow rates prior to Cluster CIMS measurement. 3) Very high concentration of nitrate ion will allow more mixed clusters to be detected, i.e.  $A_m^- \cdot B_j \cdot \text{HNO}_3$ . Our measurements indicate that the stability of these clusters also depends on RH. 4) Prior to entering into the vacuum region of the Cluster CIMS, the ions pass through a curtain gas flow consisting of 200 sccm of nitrogen. This flow slightly exceeds the flow into the mass spectrometer and may might cause ion clusters to evaporate. More information on cluster chemistry can be gained by studying how these factors alter observed clusters and their concentrations.

#### S4. Modeled reactions and parameters

The modeled reactions can be divided into three categories: neutral cluster formation, chemical ionization and ion decomposition, and IIC. Table S2 lists all the reactions that were modeled. The neutral cluster forward rate constants,  $k$ , were assumed to be  $4 \times 10^{-10} \text{ cm}^3 \text{ s}^{-1}$ , and the ion forward rate constants,  $k_c$ , were taken to be  $2 \times 10^{-9} \text{ cm}^3 \text{ s}^{-1}$ . Some error is introduced in these forward rate constants but is likely small compared to other sources of uncertainty such as evaporation or decomposition rates. To constrain the number of parameters, we assumed ions either instantly decompose or do not decompose at all. Decomposition rate constants listed as *fast* were assumed to be instantaneous and the intermediate products do not form in appreciable quantities. Ion decomposition rate constants listed as  $E_{A,B^-}$  were assumed to be zero.

Table S1 provides the neutral cluster evaporation rates used for the model that produced good agreement with our observations. We examined numerous sets of neutral and ion evaporation rate combinations to determine if our measured signal ratios as a function of CI reaction time for the diamines could be explained by simple changes in evaporation rates. However, no sensible combination reproduced our observations, leading us to believe that some fraction of  $[\text{N}_2]$  with diamines is not chemically ionized by nitrate.

These evaporation rates are by no means the “correct” rates. Our model only considered clusters up to size 4. The dynamics of the larger clusters likely effect the apparent evaporate rates of the smaller clusters. The evaporation rates also indicate that the clusters have lifetimes on the order of neutral reaction time of 3 s. Therefore, we cannot say with confidence that one of these four bases will stabilize clusters more than the others: they behave similarly during the 3 s reaction time. In addition, the evaporation rates are interconnected in the complex series of cluster balance equations. Different types of experiments, ones more sensitive to small differences in slow evaporation rates, are required to better quantify evaporation, decomposition, and partial chemical ionization rates.

Table S1 List of evaporation rates used for the model

Base	$E_1 \text{ (s}^{-1}\text{)}$	$E_{2B} \text{ (s}^{-1}\text{)}$	$E_2 \text{ (s}^{-1}\text{)}$	$E_{3A3B} \text{ (s}^{-1}\text{)}$	$E_{3A3B2} \text{ (s}^{-1}\text{)}$
DMA	0.1	0	0	1	1
EDA	5	0	0	0	0
Put	5	0	0	0	0
TMEDA	5	0	0	0	0

Table S2 Summary of all the reactions modeled in this study. Note, reactions are unbalanced and written in shorthand.

Neutral cluster formation	CI and ion decomposition reactions	IIC reactions
$A_1 + B \xrightleftharpoons[E_1]{k} AB$	$A_2B_2 + NO_3^- \xrightarrow{k_c} A_2B_2^- \xrightarrow{fast} A_2^-$	$A_1^- + A_1 \xrightarrow{k_c} A_2^-$
$AB + A_1 \xrightarrow{k} A_2B$	$AB + NO_3^- \xrightarrow{k_c} AB^- \xrightarrow{fast} A_1^-$	$A_2^- + A_1 \text{ or } AB \xrightarrow{k_c} A_3^-$
$AB + AB \xrightarrow{k} A_2B_2$	$A_1 + NO_3^- \xrightarrow{k_c} A_1^-$	$A_1^- + A_2B \xrightarrow{k_c} A_3B^-$
$A_2B + B \xrightarrow{k} A_2B_2$	$A_2B + NO_3^- \xrightarrow{k_c} A_2B^- \xrightarrow{fast} A_2^-$	$A_1^- + A_3B \xrightarrow{k_c} N_4^-$
$A_2B + A_1 \xrightarrow{k} A_3B$	$A_3B + NO_3^- \xrightarrow{k_c} A_3^-B \xrightarrow{E_{A_3B^-}} A_2^- + A_1B$	$A_1^- + A_2B_2 \xrightarrow{k_c} A_3B_2^-$
$A_3B + B \xrightarrow{k} A_3B_2$	$N_4 + NO_3^- \xrightarrow{k_c} N_4^-$	$A_1^- + AB \xrightarrow{k_c} A_2B^- \xrightarrow{fast} A_2^-$
$A_3B_2 + B \xrightarrow{k} A_3B_3$	$A_3B_3 + NO_3^- \xrightarrow{k_c} A_3^-B_3 \xrightarrow{fast} A_3^-B_2$	
$A_2B_2 + A_1 \xrightarrow{k} A_3B_2$	$A_3B_2 + NO_3^- \xrightarrow{k_c} A_3^-B_2 \xrightarrow{E_{A_3B_2^-}} A_3^-B^-$	
$A_2B + AB \xrightarrow{k} A_3B_2$		
$A_2B_2 + AB \xrightarrow{k} A_3B_3$		
$A_3B_2 \xrightarrow{E_{A_3B_2}} A_2B_2 + A_1$		
$A_3B \text{ or } A_3B_2 \text{ or } A_3B_3 + AB \xrightarrow{k} N_4$		
$A_3B_2 \text{ or } A_3B_3 + A_1 \xrightarrow{k} N_4$		
$A_2B_2 \xrightarrow{E_2} AB + AB$		
$A_2B_2 \xrightarrow{E_{2B}} A_2B + B$		
$A_3B \xrightarrow{E_{A_3B}} A_2B + A_1$		

## References:

- Berresheim, H., Elste, T., Plass-Dülmer, C., Eisele, F. L., and Tanner, D. J.: Chemical ionization mass spectrometer for long-term measurements of atmospheric OH and H<sub>2</sub>SO<sub>4</sub>, *International Journal of Mass Spectrometry*, 202, 91-109, 10.1016/s1387-3806(00)00233-5, 2000.
- Eisele, F. L., and Hanson, D. R.: First Measurement of Prenucleation Molecular Clusters, *The Journal of Physical Chemistry A*, 104, 830-836, 10.1021/jp9930651, 2000.
- Rosser, S., and de la Mora, J. F.: Vienna-Type DMA of High Resolution and High Flow Rate, *Aerosol Science and Technology*, 39, 1191-1200, 10.1080/02786820500444820, 2005.
- Ude, S., and de la Mora, J. F.: Molecular monodisperse mobility and mass standards from electrosprays of tetra-alkyl ammonium halides, *Journal of Aerosol Science*, 36, 1224-1237, 10.1016/j.jaerosci.2005.02.009, 2005.
- Zhao, J., Eisele, F. L., Titcombe, M., Kuang, C., and McMurry, P. H.: Chemical ionization mass spectrometric measurements of atmospheric neutral clusters using the cluster-CIMS, *J. Geophys. Res.*, 115, D08205, 10.1029/2009jd012606, 2010.